

## Atomic Current across an Optical Lattice

Alexey V. Ponomarev,<sup>1,2</sup> Javier Madroñero,<sup>1,3</sup> Andrey R. Kolovsky,<sup>1,2</sup> and Andreas Buchleitner<sup>1</sup>

<sup>1</sup>Max-Planck-Institut für Physik komplexer Systeme, Nöthnitzer Straße 38, 01187 Dresden, Germany

<sup>2</sup>Kirensky Institute of Physics, 660036 Krasnoyarsk, Russia

<sup>3</sup>Physik Department, Technische Universität München, James-Frank-Straße, 85747 Garching, Germany

(Received 23 September 2005; published 9 February 2006)

We devise a microscopic model for the emergence of a collision-induced, fermionic atomic current across a tilted optical lattice. Tuning the—experimentally controllable—parameters of the microscopic dynamics allows us to switch from Ohmic to negative differential conductance.

DOI: 10.1103/PhysRevLett.96.050404

PACS numbers: 03.75.Lm, 03.65.Yz, 03.75.Mn, 05.30.-d

Ultracold atoms in optical potentials provide a versatile tool for the experimental study of many-body dynamics, with an unprecedented degree of accuracy [1–3]. Not only do these systems allow the faithful experimental realization of fundamental model Hamiltonians of solid state theory, but they also lend themselves as efficient analog quantum simulators [4]. Beyond that, they bridge the gap between the single particle and the thermodynamic limit: if not now, certainly so in the near future experimentalists will be able to load a precisely controlled number of particles into engineered potentials, with particle numbers tunable from one to intermediate or large values [5]. Hence, by continuously varying the system size, we will be able to control the emergence of macroscopic, thermodynamic observables from perfectly deterministic Hamiltonian dynamics, in experiment and theory. This holds the potential of a much deeper and quantitative understanding of quantum statistical laws, together with a variety of possible applications in the context of the ever advancing miniaturization of modern technology [6].

In the present contribution, we address a specific problem of exemplary importance within this context: the emergence of a macroscopic current across a periodic potential under static forcing. It is well known that electrons in a perfectly periodic lattice exhibit coherent Bloch oscillations, under static forcing, and that no net transport, i.e., no current across such lattice, occurs in the absence of any (incoherent or dephasing) relaxation process [7]. Only the latter will induce a net drift velocity of the electrons, giving rise to a measurable current. While relaxation processes due to phonon scattering or impurities are abundant yet largely uncontrolled in solids, a clean and perfectly controllable realization of this fundamental transport problem is feasible in a quantum optical setting, where we can engineer the environment: By loading spin polarized, non-interacting fermions together with ultracold bosons into a one-dimensional optical lattice, we establish a strictly analogous, idealized scenario. The bosons act as a bath for the fermions, with relaxation induced by fermion-boson collisions.

Our results are obtained from a microscopic model for very moderate system sizes—typically less than ten bo-

sons interacting with a single fermion, on approximately ten lattice sites. Yet, due to the exponential increase of the many particle system's Hilbert space dimension with particle number and lattice size, this is sufficient to enter the regime of asymptotic convergence into the thermodynamic limit [8]. Thus, we describe how a macroscopic current emerges from perfectly Hamiltonian microscopic dynamics, with all ingredients under essentially perfect experimental control.

Our model Hamiltonian reads

$$H = H_F + H_B + H_{\text{int}}, \quad (1)$$

and decomposes into the (single-particle) fermionic part

$$H_F = -\frac{J_F}{2} \left( \sum_l |l+1\rangle\langle l| + \text{H.c.} \right) + Fd \sum_l |l\rangle\langle l|, \quad (2)$$

the (many particle) bosonic part

$$H_B = -\frac{J_B}{2} \left( \sum_l \hat{a}_{l+1}^\dagger \hat{a}_l + \text{H.c.} \right) + \frac{W_B}{2} \sum_l \hat{n}_l (\hat{n}_l - 1), \quad (3)$$

and a term which mediates the collisional interaction between fermions and bosons,

$$H_{\text{int}} = W_{FB} \sum_l \hat{n}_l |l\rangle\langle l|. \quad (4)$$

Since we are interested in the fermionic dynamics, the fermionic tunneling coupling  $J_F$  in (2) sets the energy scale, and, correspondingly,  $\hbar/J_F$  is the natural unit of time. Equations (1)–(4) describe the dynamics of ultracold atoms in the lowest band of a 1D lattice, assuming short range (on-site) interaction, and tunneling coupling only between adjacent lattice sites  $l$ . Low temperatures as well as moderate field strengths as compared to the gap between the lattice's lowest and first excited bands are required, for consistency with the single band approximation. The single-particle ansatz for the fermionic part is justified since the Pauli principle forbids occupation of the same site. Our model additionally implies that only fermions experience a static forcing  $F$ , while the bosons see a periodic potential (period  $d$ ) without static forcing. Such a situation can be realized by a suitable choice of the internal electronic states the fermions and bosons are initially prepared in [9].

We impose  $J_B = J_F$  for the bosonic component and focus on filling factors  $\bar{n} = N/L \sim 1$  with  $N$  bosons distributed over  $L$  lattice sites (for more than one fermion,  $N$  represents the boson number per fermion). These filling factors interpolate between single-particle dynamics and the thermodynamic limit, for the lattice sizes we consider. The above choice of parameters is in reach for state-of-the-art experiments:  $J_B \simeq J_F/2$  has already been realized in experiments [10] on a mixture of  $^{40}\text{K}$  and  $^{87}\text{Rb}$ , with  $J_F \simeq 0.06E_R$ , and experimental techniques for the relative adjustment of  $J_F$  and  $J_B$  are available [4,9,11]. Here,  $E_R = \hbar^2 k^2 / 2m$  is the single photon recoil energy seen by the  $^{40}\text{K}$  atoms. With the above value of  $J_F$ , the relevant time scale  $\hbar/J_F \simeq 0.3$  s is easily resolved. Finally, for our subsequent theoretical/numerical treatment, the total dimension  $\mathcal{N}$  of the Hilbert space scales as  $\mathcal{N} = L\mathcal{N}_B$ , where  $\mathcal{N}_B = (N + L - 1)! / N!(L - 1)!$  is the dimension of the bosonic subspace. The exponential increase of  $\mathcal{N}$  with  $N_B$  and  $L$  is thus evident.

In the absence of interactions between the fermionic and bosonic component [ $W_{FB} = 0$  in (4)], the fermions will undergo coherent Bloch oscillations with a period  $T_B = 2\pi\hbar/Fd$  [7]. However, finite values of  $W_{FB}$  will induce a collision-induced relaxation of the fermionic dynamics, eventually resulting in a nonvanishing current across the lattice. For weak coupling between fermions and bosons, we can describe the reduced fermionic dynamics in second order perturbation theory in  $W_{FB}$ . Further, we use the fact that the bosonic subsystem is known to exhibit chaotic level statistics (in the random matrix sense), over a broad range of  $W_B$  and  $J_B$  [8,12], and therefore can substitute for a noisy environment [13], provided its initial state is characterized by equally distributed populations of the different sublevels (this is the high-temperature limit on the scale of the lattice's lowest band's energy spread, though perfectly compatible with keeping low temperatures on the scale of the gap between the lattice's fundamental and first excited band). Indeed, the boson-number cross-correlation function,

$$R_{l,m}(t, t') = \text{Tr}[\hat{n}_l(t)\hat{n}_m(t')], \quad (5)$$

$$\hat{n}_l(t) = \exp(iH_B t/\hbar)\hat{n}_l \exp(-iH_B t/\hbar),$$

is very well approximated by the cross correlation generated by a random matrix Hamiltonian (chosen from the Gaussian orthogonal ensemble [12]), as illustrated in Fig. 1 for  $R_{1,1}(t, 0)$  and  $R_{1,2}(t, 0)$ . For  $N > 2$  and  $L$  such that  $\mathcal{N}_B > 100$ , we numerically extract a well-defined, finite time scale  $\tau \simeq 3\hbar/J_B$  for the decay of these correlations [14].

Consequently, if we choose lattice constant  $d$  and static field strength  $F$  such that  $\tau \ll T_B$  [15], the correlation function of the bath can be approximated by a  $\delta$  function

$$R_{l,m}(t, t') = \bar{n}^2 \delta_{l,m} \delta\left(\frac{t-t'}{\tau}\right), \quad (6)$$

on the typical time scale of the fermionic dynamics, given by the Bloch period  $T_B$ . This justifies a Markov approxi-

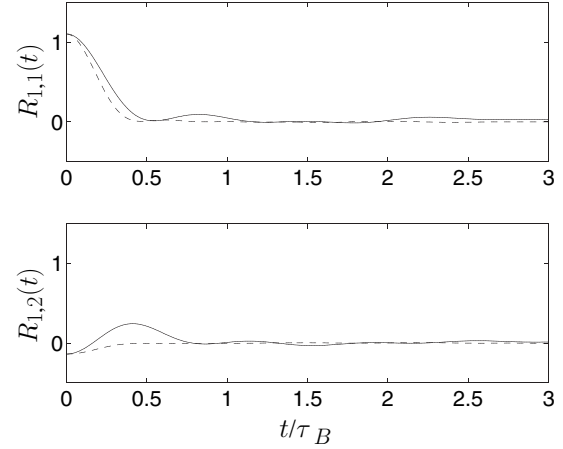


FIG. 1. Time evolution of the number correlation functions  $R_{1,1}(t, 0)$  (top panel) and  $R_{1,2}(t, 0)$  (bottom panel) of the bosonic bath (3), initially prepared in an equally weighted superposition of the bosonic eigenstates.  $N = 7$ ,  $L = 9$ . The ratio between interatomic interaction strength and tunneling coupling is fixed at  $W_B/J_B = 3/7$ , what ensures that we are in the parameter range of Wigner-Dyson spectral statistics, at  $\bar{n} \simeq 1$  [8]. Time is measured in units of the site-to-site tunneling period  $\tau_B = \hbar/J_B$ . The dashed lines show the bosonic correlation functions which result from substituting the Bose-Hubbard Hamiltonian (3) by a random matrix of the Gaussian orthogonal ensemble.

mation after tracing out the bosonic degrees of freedom, and we end up with the master equation for the fermionic density matrix,

$$\frac{\partial \rho_{l,m}^{(F)}}{\partial t} = -\frac{i}{\hbar} [H_F(t), \rho^{(F)}]_{l,m} - \gamma(1 - \delta_{l,m})\rho_{l,m}^{(F)}, \quad (7)$$

where the decay rate is given by

$$\gamma = \frac{\tau \bar{n}^2 W_{FB}^2}{\hbar^2} \simeq \frac{3\bar{n}^2 W_{FB}^2}{\hbar J_B}. \quad (8)$$

An analytic solution [16] of (7) leads to the following expression for the mean fermionic velocity in the lattice:

$$v(t) = v_0 e^{-\gamma t} \sin(\omega_B t), \quad v_0 = \frac{J_F d}{\hbar}, \quad \omega_B = \frac{F d}{\hbar}, \quad (9)$$

in perfect agreement with the numerical result obtained from a direct propagation of the dynamics, with the bosonic bath prepared in an equally weighted statistical mixture of the eigenstates of the Bose-Hubbard Hamiltonian (equivalent to the high-temperature limit), while the fermionic subsystem is launched in a Bloch wave with vanishing quasimomentum. As illustrated in Fig. 2, the fermionic Bloch oscillations decay irreversibly, with a decay constant  $\gamma$  which—in agreement with Eq. (8)—is fully controlled by the filling factor  $\bar{n}$ , by the fermion-boson interaction strength  $W_{FB}$ , and by the bosonic tunneling coupling  $J_B$ .

However, Fig. 2 indicates no nonvanishing average drift of the fermions across the lattice; hence no current is observed. This is a consequence of our above derivation: while the master equation description provides a quite

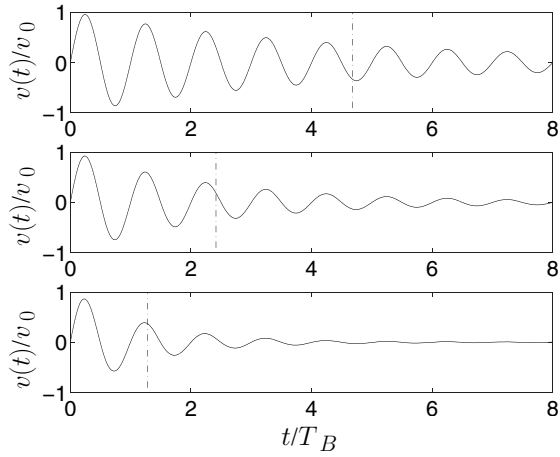


FIG. 2. Normalized mean velocity of the Fermi atoms, in units of  $v_0 = J_F d/\hbar$  for  $Fd = 0.57 \times J_F$ ,  $J_B = J_F$  for fermion-boson interaction strengths  $W_{FB} = 0.101 \times J_F$ ,  $0.143 \times J_F$ ,  $0.202 \times J_F$  (from top to bottom), and  $N = 7$ ,  $L = 9$ . The typical time scale of the interaction induced decay of the fermionic Bloch oscillations fits the time scale  $\gamma^{-1}$  predicted by Eq. (8) (dash-dotted vertical lines) very well. The same observation holds for fixed  $W_{FB}$  and variable  $Fd$  (not shown here).

satisfactory and quantitative picture of the collision-induced decoherence of the fermionic Bloch oscillations, it also implies that there is no backaction of the fermion-boson coupling on the bath (this is the essence of the Markov approximation). Consequently, no net energy can be transferred from the fermionic into the bosonic component (the latter being initially in a fully thermalized state), as clearly manifest in the time evolution of the average energy of the bosonic component, represented by the dashed line in the bottom panel of Fig. 3. If instead we choose a bosonic initial condition given by a low temperature Boltzmann distribution  $P(\epsilon_i) \sim \exp(-\epsilon_i/k_B T)$ , with temperature  $k_B T \approx 2.86 \times J_B$  [17], over its energy levels  $\epsilon_i$ , the bath can be heated by the collisions with the fermions, and thus extract energy from the fermionic component. Such a choice of the bosonic initial state leads to the relaxation of the fermionic Bloch oscillations, associated with a (non-Markovian) energy increase of the bosonic component; see Fig. 3. Correspondingly, the fermionic mean velocity exhibits a nonvanishing drift, on top of the oscillatory behavior due to the Bloch dynamics. A finite fermionic current across the lattice is observed in the upper panel of Fig. 3. Since we will be dealing with a closed system of finite size (finite particle number and finite lattice length), the bosonic bath has a finite heat capacity and cannot act as a reservoir over arbitrary time scales. Consequently, the relaxation-induced current ceases as soon as the bath is fully thermalized by draining energy from the fermionic dynamics.

#### Fermionic drift

$$\bar{v}(t) = v(t) - v_0 e^{-\gamma t} \sin(\omega_B t) \quad (10)$$

and bosonic energy gain  $\Delta E_B$  are related through the

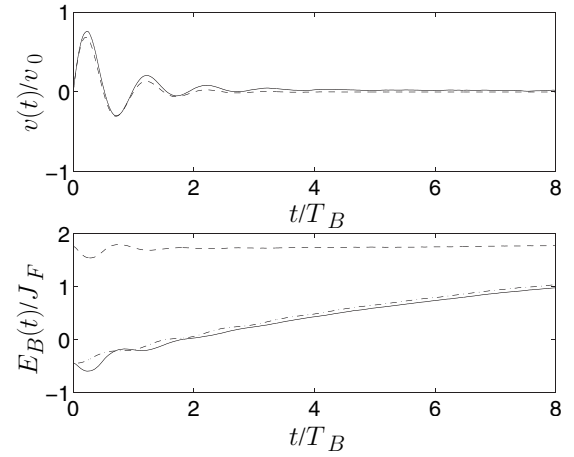


FIG. 3. Mean velocity  $v(t)$  of the fermionic component (top panel, solid line), in units of  $v_0 = J_F d/\hbar$ , and average energy  $E_B(t)$  of the bosonic component (bottom panel, solid line), in units of  $J_F$ , for a low temperature ( $k_B T \approx 2.86 \times J_B$ ) initial state of the bosonic bath.  $Fd = 0.143 \times J_F$ ,  $W_{FB} = 0.143 \times J_F$ ,  $W_B/J_B = 3/7$ ,  $J_B = J_F$ ,  $N = 7$ ,  $L = 9$ . The dashed lines indicate the corresponding solutions for a thermalized initial state of the bath,  $k_B T \approx 150 \times J_B$ . For a nonequilibrium initial condition of the bath the finite drift velocity  $\bar{v}(t)$  manifests as a clear, nonvanishing offset of the fermionic mean velocity with respect to the Markovian result indicated by the dashed line (top panel). The dash-dotted line in the bottom plot is obtained by integration of Eq. (11).

classical relation  $\Delta E_B = F \Delta x = F \bar{v} \Delta t$ , i.e.,

$$\frac{\partial E_B}{\partial t} = F \bar{v}(t). \quad (11)$$

Integration of (11) with  $\bar{v}$  as defined in (10), together with  $v(t)$  from the exact solution of the Schrödinger equation under (1), leads to a very good fit of the exact time dependence of the bosonic mean energy, in the lower panel of Fig. 3. We can thus deduce the current-voltage characteristics for the fermions, i.e., the dependence of the drift velocity  $\bar{v}$  (equivalent to the current, modulo the carrier density) on the static force (or potential difference across the lattice) which generates the current: For sufficiently short times, Eq. (11) can be rewritten as  $\Delta E_B = F \bar{v} \Delta t$ , where  $F \bar{v}$  can be extracted from the exact result for  $E_B(t)$  as displayed in Fig. 3 (averaging over the residual Bloch oscillations during the first two Bloch cycles). Dividing this initial growth rate of  $E_B(t)$  by  $F$ , we obtain the dependence of the “current”  $\bar{v}$  on the “voltage”  $F$  in Fig. 4, which exhibits a marked transition from Ohmic ( $\bar{v} \sim F$ ) behavior to negative differential conductivity ( $\bar{v} \sim 1/F$ ), as  $F$  is increased. Remarkably, this faithfully reproduces the qualitative behavior predicted by the phenomenological Esaki-Tsu relation [18] for a current across doped superlattices,

$$\bar{v} = \frac{v_0}{4} \frac{\omega_B/\gamma}{1 + (\omega_B/\gamma)^2}, \quad (12)$$

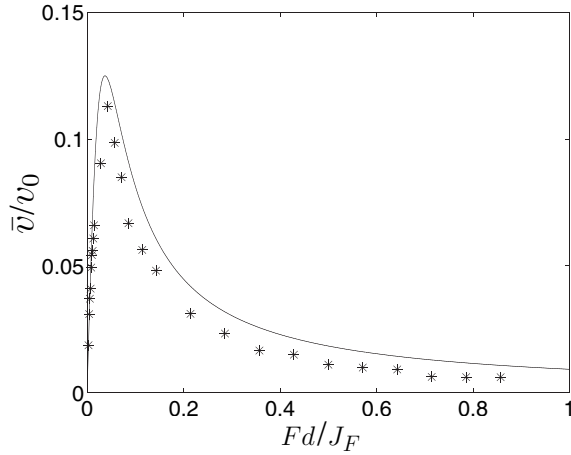


FIG. 4. Fermionic drift velocity  $\bar{v}$  (stars), in units of  $v_0 = J_F d/\hbar$ , vs static forcing  $Fd$ , in units of  $J_F$ , compared to the prediction of Eq. (12) (continuous line), for the same parameters. The Bloch frequency  $\omega_B = Fd/\hbar$  increases with  $F$ , while the effective decay rate  $\gamma \approx 0.037J_F/\hbar$ , derived from (8) for  $N = 7$ ,  $L = 9$ ,  $W_{FB} = 0.143 \times J_F$ ,  $W_B/J_B = 3/7$ ,  $J_B = J_F$ , is constant. Note the clear transition from Ohmic ( $\bar{v} \sim Fd$ ) to negative differential conductance ( $\bar{v} \sim 1/Fd$ ), at a finite value of  $Fd$ .

with quantitative differences, notably for large  $F$ , due to the finite size of our atomic sample. Note that, in contrast to experiments in semiconductor superlattices, the effective scattering rate  $\gamma$  is perfectly controlled and continuously tunable (e.g., via Feshbach resonances [19]) in our present quantum optical setting, as a consequence of Eq. (8).

In conclusion, we have shown that a directed current of spin-polarized ultracold fermionic atoms across a one-dimensional optical lattice under static forcing can be induced by collisional interaction with a bosonic admixture. While the current increases linearly with the static force in the limit where the collision-induced decay rate (independent of the static forcing) is much larger than the fermionic Bloch frequency (increasing linearly with the static field strength), it decreases inversely proportional to  $F$  in the opposite limit. This crossover has an intuitive cause: Finite, collision-induced decay rates induce diffusive transport at arbitrarily weak forcing (many collision events during one Bloch cycle), while strong forcing and small collision rates (few collisions during many Bloch cycles) essentially reestablish the Bloch oscillations and suppress the directed current.

Our theory, based on a microscopic, strictly Hamiltonian picture of the many-body dynamics, is amenable to experimental scrutiny. It also identifies the microscopic origin of first experimental observations which already pointed in this direction, on the basis of a purely phenomenological interpretation [1]. Furthermore, our model allows for bosonic baths composed of an arbitrary number of particles. Future work will explore the limit of very small baths, with small Hilbert space dimensions and a reduced density of

states. In this regime, non-Markovian effects due to the granularity of the bath are expected, which will be in reach for direct experimental probing. Finally, the generalization of our work to 2D geometries, where also magnetic field effects may be included [20], could open new avenues to study complex or chaotic [21] fermionic transport with tunable relaxation rates.

We acknowledge fruitful discussions with Artem Dudarev, and partial financial support by Deutsche Forschungsgemeinschaft, within the SPP1116 program.

- 
- [1] H. Ott, E. de Mirandes, F. Ferlaino, G. Roati, G. Modugno, and M. Inguscio, *Phys. Rev. Lett.* **92**, 160601 (2004).
  - [2] B. Paredes, A. Widera, V. Murg, O. Mandel, S. Fölling, I. Cirac, G. V. Shlyapnikov, T. W. Hänsch, and I. Bloch, *Nature (London)* **429**, 277 (2004).
  - [3] M. Köhl, H. Moritz, T. Stöferle, K. Günter, and T. Esslinger, *Phys. Rev. Lett.* **94**, 080403 (2005).
  - [4] D. Jaksch and P. Zoller, *Ann. Phys. (N.Y.)* **315**, 52 (2005).
  - [5] C.-S. Chuu, F. Schreck, T. Meyrath, J. Hanssen, G. Price, and M. Raizen, *Phys. Rev. Lett.* **95**, 260403 (2005).
  - [6] J. Fortágh and C. Zimmermann, *Science* **307**, 860 (2005).
  - [7] P. W. Anderson, *Concepts in Solids: Lectures on the Theory of Solids* (Addison-Wesley, New York, 1992).
  - [8] A. Kolovsky and A. Buchleitner, *Europhys. Lett.* **68**, 632 (2004).
  - [9] Y. Takasu, K. Maki, K. Komori, T. Takano, K. Honda, M. Kumakura, T. Yabuzaki, and Y. Takahashi, *Phys. Rev. Lett.* **91**, 040404 (2003).
  - [10] G. Modugno, F. Ferlaino, R. Heidemann, G. Roat, and M. Inguscio, *Phys. Rev. A* **68**, 011601(R) (2003).
  - [11] M. Takamoto and H. Katori, *Phys. Rev. Lett.* **91**, 223001 (2003).
  - [12] O. Bohigas, in *Chaos and Quantum Physics*, Proceedings of the Les Houches Summer School, Session LII, edited by M.-J. Giannoni, A. Voros, and J. Zinn-Justin (North-Holland, Amsterdam, 1991), p. 87.
  - [13] A. R. Kolovsky, *Phys. Rev. E* **50**, 3569 (1994).
  - [14] For smaller particle numbers and/or lattice sizes, the bath correlations exhibit (partial) revivals on short time scales which become comparable to the typical time scales we consider here. Hence, in this limit, finite size effects would invalidate our subsequent Markovian treatment.
  - [15] The latter implies  $Fd \ll 2\pi J_B/3$ , by virtue of the definitions of  $\tau$  and  $T_B$ , and is thus compatible with our earlier choices  $Fd < J_F$  and  $J_B = J_F$ .
  - [16] A. R. Kolovsky, A. V. Ponomarev, and H. J. Korsch, *Phys. Rev. A* **66**, 053405 (2002).
  - [17] It is possible to show that  $|\epsilon_i| \leq NJ_B$ , in the limit  $W_{FB} \rightarrow 0$  [8].
  - [18] L. Esaki and R. Tsu, *IBM J. Res. Dev.* **14**, 61 (1970).
  - [19] S. Inouye, M. R. Andrews, J. Stenger, H. J. Miesner, D. M. Stamper-Kurn, and M. Ketterle, *Nature (London)* **392**, 151 (1998).
  - [20] G. Juzeliūnas, P. Öhberg, J. Ruseckas, and A. Klein, *Phys. Rev. A* **71**, 053614 (2005).
  - [21] T. Fromhold *et al.*, *Nature (London)* **428**, 726 (2004).